APPLICATION OF A TENSOR INTERPOLATION METHOD ON THE DETERMINATION OF FIBER ORIENTATION TENSORS FROM COMPUTED TOMOGRAPHY IMAGES

Juliane Blarr[a], Noah Kresin[a], Constantin Krauß[b], Kay A. Weidenmann[c,d], Wilfried V. Liebig[a,d], Peter Elsner[a,d]

a: juliane.blarr@kit.edu, Karlsruhe Institute of Technology (KIT), Institute for Applied Materials (IAM-WK), Hybrid and Lightweight Materials, Engelbert-Arnold-Straße 4, 76131 Karlsruhe, Germany
b: Karlsruhe Institute of Technology (KIT), Institute of Vehicle System Technology - Division Lightweight Technology, Rintheimer Querallee 2, 76131 Karlsruhe, Germany
c: Universität Augsburg, Institute of Materials Resource Management, Universitätsstr. 2, 86159 Augsburg
d: Fraunhofer Institute for Chemical Technology ICT, Joseph-von-Fraunhofer Strasse 7, 76327 Pfinztal, Germany

Abstract: *When investigating the mechanical behavior of fiber-reinforced polymers, fiber orientation plays a decisive role concerning anisotropy. Fiber orientation distributions are typically measured in the form of fiber orientation tensors. In order to measure orientation tensors, computed tomography scans and consecutive image processing methods have become one of the leading non-destructive testing methods. The conflict between scan resolution and sample size limits the volume that can be scanned. To obtain the fiber orientation behavior across an entire plate, a direct interpolation of orientation tensors computed from CT scans of smaller volumes at selected coordinates of the plate is implemented. Rather than a component-based interpolation, the authors chose a decomposition and reassembly method interpolating shape and orientation of the tensors separately. While this approach has been implemented and used for e.g. diffusion tensors in medical imaging, the authors consider the application to sparse but measured CT-based data to be a novelty.*

Keywords: tensor mapping; tensor algebra; quaternions; non-destructive testing; image processing

1. Introduction and state of the art

Fiber orientation distributions (FOD) are one of the various characteristic quantities evolved over time in order to quantify the microstructure of long- and short-fiber-reinforced polymers (FRP). Fiber orientation specifically has a high impact on anisotropy as the fiber orientation is typically a function of the position since orientation is defined by process (compression molding) induced material flow. FOD are described in scalar distribution functions. However, in the use cases of process or structural simulations the most common and compact form of representation are fiber orientation tensors (FOT) [1]. FOT can be determined from µCT images via structure tensor approach [2]. While fiber volume contents (FVC) and fiber length distributions (FLD) can also be determined experimentally by eliminating the matrix material [3], validating FOT determined via image processing depicts a challenge. Furthermore, the conflict

  doi:10.5075/epfl-298799_978-2-9701614-0-0

between image resolution and sample size in CT images limits the volume that can be scanned in order to still detect carbon fibers (diameter of 5 µm - 7 µm) massively. These small volumes often do not represent the microstructure sufficiently well and additionally, the coverage of a full plate is resource-intensive. However, full-field information on FOT is of elevated interest when analyzing and trying to improve the preceding manufacturing process and corresponding process simulation. The alternative to a high amount of scans and orientation analyses, i.e. considering less measured tensors and ascertaining predicted values in between, constitutes a classical interpolation problem. While interpolation for scalar values is well-known and various approaches exist, interpolation of tensors represents a more challenging, less well-explored field. The fact that orientation tensors are received via closure approximations of the orientation distribution function (ODF) might be considered as an advantage. A scalar interpolation for discrete directions is thereby possible (e.g. in contrast to strain or stress tensors). The easiest way of interpolating fiber orientations would then be a Euclidean interpolation of the scalar valued function $\bar{\phi}$. The result is a weighted arithmetic averaging of the tensor components. Interpolating the tensor components lead to a kind of "shape shift" instead of sufficient rotation of the interpolated tensors in former studies, particularly showing an "artificial" isotropy [4-6]. There are further "global" interpolation methods, which could be applied to symmetric positive-definite (SPD) tensors. The Riemannian Interpolation has been used e.g. in [7]. However, as soon as more than two input arguments are used, the underlying computations can only be solved implicitly, necessitating an iterative and computationally expensive method, which is why this method is not pursued any further in this work. As another logarithmic, yet explicitly solvable approach, Arsigny et al. [4] introduced the Log-Euclidean tensor interpolation method. As a completely different kind of concept, decomposition-based methods have been made use of. These approaches are grounded on the idea of the generally acknowledged spectral decomposition of tensors (cf. Eq. (3)). This is followed by a separate interpolation of shape (e.g. invariants like Eigenvalues) and of orientation (e.g. Eigenvectors or quaternions) and a subsequent reassembly to a then interpolated tensor. This method particularly provides the possibility of a smoother behavior in-between two differently oriented tensors and has been used successfully for diffusion tensors in medical imaging [5]. However, the specific interpolation of shape and orientation can be realized in multiple, different ways. The chosen methods for the implementation of the decomposition method in this work are explained in detail in the "Methods" chapter. Sabiston et al. [8] have explored the use of artificial intelligence (AI) for FOT interpolation. The authors used ground truth fiber orientation data from µCT measurements - as also used in this work. They then trained an artificial neural network with this data, which was subsequently able to predict tensor components within ranges smaller than the variability of the orientation of neighboring microstructural units.

This work focuses on determining a full-field distribution of fiber orientation tensors across an entire carbon long-fiber-reinforced polyamide 6 plate by interpolating orientation tensors determined from small samples at specific positions. Therefore, nine samples were scanned in the CT and the orientation tensor was determined for each scanned volume. Following, the nine computed tensors of second order were interpolated via a decomposition-based interpolation method and the results were discussed both visually and quantitatively with the help of the Frobenius norm.

  doi:10.5075/epfl-298799_978-2-9701614-0-0

2. Notation

Symbolic tensor notation is preferred in this work. Scalar values are denoted by standard Latin and Greek letters, e.g. c, λ. Tensors of first order are represented by bold lowercase letters, e.g. $\boldsymbol{x}, \boldsymbol{p}$ and bold uppercase letters are used for tensors of second order such as $\boldsymbol{R}, \boldsymbol{S}$. Fourth-order tensors are denoted by double-struck letters like $\mathbb{C}, \mathbb{S}$.

Sets, i.e., collections of quantities, are denoted by calligraphic symbols, e.g. $\mathcal{A}$ and are constructed by curly braces. In them, the elements typically are given explicitly or expressed by conditions to be fulfilled by each element contained in the set. The special orthogonal group $SO(3)$ represents all 3D rotations. Four-dimensional quaternions are represented by an arrow-head above the Latin letter, such as in $\vec{q}$.

The terms $tr()$ and $det()$ are the trace and determinant operators respectively, $|\boldsymbol{D}|$ represents the Frobenius norm of the tensor $\boldsymbol{D}$ defined by $|\boldsymbol{D}| = \sqrt{tr(\boldsymbol{D}\boldsymbol{D}^T)}$. The rotation of a tensor is denoted by the Rayleigh Product ★.

3. Methods

4.1 General

The interpolation method was mainly implemented in Python 3.8. SPD tensors can be visualized as tensor glyphs [9]. This method was used in this work as it constitutes a descriptive and interpretable way of assessing the success of the implemented interpolation method. The authors implemented the visualization in Matlab R2020b with the help of the “plotDTI” function of the fanDTasia ToolBox by Barmpoutis et al. [10].

4.2 Scan acquisition and determination of fiber orientation tensors

The authors used the YXLON-CT precision µCT system with a flat panel PerkinElmer Y.XRD1620 detector with 2048 px x 2048 px. 1950 projections were made per scan and an accelerating voltage of 150 kV and a current of 0.25 mA were chosen with an integration time of 500 ms and a frame binning of two. The resulting volumetric images are reconstructed applying the Feldkamp cone-beam algorithm [11]. The scans had a voxel size of 0.00857123 mm/voxel.

In this study, carbon fiber-reinforced polyamide 6 is investigated. This material is manufactured in the so-called "long-fiber thermoplastic direct process" (LFT-D) introduced by Krause et. al [12]. This is a compression molding process in which a so-called plastificate, an elongated, cross-sectionally oval mix of C-fibers and polymer blend, comes out of the extruder and is placed sideways in a press, which then closes in and produces CF-PA6 plates. Out of one of these manufactured plates, which have dimensions of 400 mm x 400 mm x 4 mm, nine samples of 10 mm x 10 mm x 4 mm were cut via waterjet cutting and scanned with the described parameters.

Subsequently, the reconstructed scans were processed in VG Studio Max 3.4.2. If necessary, brightness and contrast were adjusted in the ImageJ (FIJI) software. In addition, the individual gray value threshold was determined for each scan. To determine the FOT from the scan data, the method introduced by Pinter et al. [13] was used. The algorithm (implemented in C++ with the help of the ITK library) makes use of the structure tensor (cf. Eq. (1)):

  doi:10.5075/epfl-298799_978-2-9701614-0-0

$$\boldsymbol{S} = \begin{bmatrix} \left(\frac{\delta I}{\delta x}\right)^2 & \frac{\delta I}{\delta x}\frac{\delta I}{\delta y} & \frac{\delta I}{\delta x}\frac{\delta I}{\delta z} \\ \frac{\delta I}{\delta y}\frac{\delta I}{\delta x} & \left(\frac{\delta I}{\delta y}\right)^2 & \frac{\delta I}{\delta y}\frac{\delta I}{\delta z} \\ \frac{\delta I}{\delta z}\frac{\delta I}{\delta x} & \frac{\delta I}{\delta z}\frac{\delta I}{\delta y} & \left(\frac{\delta I}{\delta z}\right)^2 \end{bmatrix} \quad (1)$$

The structure tensor calculation is combined with a Gaussian blur of a width of $\sigma = 0.2$ and a mask size of 2. The FOT calculated with this algorithm constitute the foundation or ground truth that is fed into the interpolation method. They are henceforth called "measured values", implicitly including that these FOT are subject to a certain error as well.

4.3 Decomposition-based interpolation method

Determining values between a set of measured values, here the set $\mathcal{T}_m = \{\boldsymbol{UL}, \boldsymbol{UM}, \boldsymbol{UR}, \boldsymbol{ML}, \boldsymbol{MM}, \boldsymbol{MR}, \boldsymbol{LL}, \boldsymbol{LM}, \boldsymbol{LR}\}$ (respectively denoting “Upper Left, Upper Middle, Upper Right, Middle Left, …, Lower Left, etc.”) of measured FOT computationally, based on the set of measured values, describes the interpolation problem at hand. An interpolation scheme $\bar{\phi}$ is defined as a mapping f, which connects its arguments, on the one hand a set of $N \geq 1$ discrete values ϕ_i and on the other hand their associated weights $w_i \in [0; 1]$: $\bar{\phi} = f(\phi_i, w_i)$. For the chosen decomposition approach, the shape and orientation of the tensors are to be interpolated separately. Therefore, the well-known spectral decomposition resulting from the Eigenvalue problem is used:

$$\boldsymbol{A} = \boldsymbol{R}\boldsymbol{\Lambda}\boldsymbol{R}^T = \boldsymbol{R} \bigstar \boldsymbol{\Lambda}. \quad (2)$$

$\boldsymbol{\Lambda}$ denotes the tensor containing the Eigenvalues on the principal diagonal and $\boldsymbol{R}$ is defined as the orthogonal rotation matrix consisting of the normalized Eigenvectors.

4.3.1 Orientation

The rotation matrix $\boldsymbol{R}$ can be interpreted as a rotation around a rotation axis and therefore be transformed into a quaternion:

$$q = \cos\frac{\theta}{2} + \left(u_x\,\boldsymbol{i} + u_y\,\boldsymbol{j} + u_z\,\boldsymbol{k}\right)\sin\frac{\theta}{2} \quad \text{with} \quad \text{rotation axis } \boldsymbol{u} = (u_x,\ u_y,\ u_z)^T \text{ and rotation angle } \theta. \quad (3)$$

Following, the quaternion is calculated from the given rotation matrix $\boldsymbol{R}$ via:

$$t = tr(\boldsymbol{R}), r = \sqrt{1+t} \quad \text{and} \quad a = \frac{r}{2} \quad \text{with}$$

$$b = sgn(R_{zy} - R_{yz})\left|\frac{1}{2}\sqrt{1 + R_{xx} - R_{yy} - R_{zz}}\right|,$$

$$c = sgn(R_{xz} - R_{zx})\left|\frac{1}{2}\sqrt{1 - R_{xx} + R_{yy} - R_{zz}}\right| \text{ and}$$

$$d = sgn(R_{yx} - R_{xy})\left|\frac{1}{2}\sqrt{1 - R_{xx} - R_{yy} + R_{zz}}\right|. \quad (4)$$

This is followed by the actual interpolation:

$$q_{ges} = \sum_i w_i\, q_i \quad \text{with weights yielding} \quad \sum_i w_i = 1. \quad (5)$$

  doi:10.5075/epfl-298799_978-2-9701614-0-0 published under CC BY-NC 4.0 license

The retransformation of the resulting quaternion in the rotation matrix $\boldsymbol{R}$ is realized with

$$\boldsymbol{R} = \begin{bmatrix} a^2+b^2-c^2-d^2 & 2(bc-ad) & 2(bd+ac) \\ 2(bc+ad) & a^2-b^2+c^2-d^2 & 2(cd-ab) \\ 2(bd-ac) & 2(cd+ab) & a^2-b^2-c^2+d^2 \end{bmatrix}. \quad (6)$$

4.3.2 Shape

For the interpolation of the shape, three linear independent invariants are formed of each tensor and interpolated separately. Of the orthogonal K- and R-invariants introduced by Ennis et al. [6] K_1, R_2 and R_3 will be used (based on the approach of Gahm et al. [5]) as they apparently work well for physical problems, instead of working on the Eigenvalues or $\boldsymbol{\Lambda}$ respectively, with $\boldsymbol{A}'$ denoting the deviatoric (anisotropic) part of $\boldsymbol{A}$:

$$K_1 = tr(\boldsymbol{A}),\ R_2 = \sqrt{\frac{3}{2}}\frac{|\boldsymbol{A}'|}{|\boldsymbol{A}|} \text{ and } R_3 = 3\sqrt{6}\det\left(\frac{\boldsymbol{A}'}{|\boldsymbol{A}'|}\right). \quad (7)$$

The invariants are then interpolated individually:

$$K_{1,ges} = \sum_i w_i K_{1,i}, \qquad R_{2,ges} = \sum_i w_i R_{2,i} \qquad \text{and} \qquad R_{3,ges} = \sum_i w_i R_{3,i}. \quad (8)$$

The authors used the following formula to calculate the associated eigenvalues from the interpolated invariants (cf. [5]):

$$\text{For } i = 1,2,3 \text{ holds: } \lambda_i = \frac{1}{3}K_1 + \frac{2K_1R_2}{3\sqrt{3-2{R_2}^2}}\cos\left(\frac{\cos^{-1}(R_3)+P_i}{3}\right) \text{ with } P_i = 0, 2\pi, -2\pi \quad (9)$$

With these Eigenvalues, Λ can then be created again. Shepard's inverse distance weighting method is used as weight function in all cases with $p = 2$: $w_i = \frac{1}{|\boldsymbol{x}_i-\boldsymbol{x}|^p}\frac{1}{\sum_j |\boldsymbol{x}_j-\boldsymbol{x}|^{-p}}$.

4. Results

The set of "measured" orientation tensors via CT scan and subsequent calculation via structure tensor $\mathcal{T}_m$ is represented by the blue tensor glyphs in Figure 1, the set of interpolated tensors $\mathcal{T}_i = \{\boldsymbol{T}_{xy}\ \forall\ x \in 1,\dots,13\ \cap y\ \in 1,\dots,13\}$ by the orange tensor glyphs. The origin of the global coordinate system is located in the lower left corner of the plate. The original LFT charge covered almost the entire left side of the 400 mm x 400 mm mold with a width of about x = 90 mm (to the right), a length of about y = 350 mm (up) and a height of about z = 60 mm. Thus, when the press closes, one would expect a quasi 1D flow to the right. However, in the picture at the top of Figure 1, a clear curve can be seen in the fiber orientation. Instead of a distinct preferred direction in the positive x-direction, the fibers align in a curve to the upper right after clear preferred direction in the left region resulting from the plastificate, i.e. from the last extrusion step in the LFT-D process. As for the interpolation method as such, the visual results are for the most part very appealing. Interpolation between the individual measured FOT is good and the transition between two adjacent tensors also appears reasonable. The anisotropy is not basically lost between two differently oriented tensors by "rounding the tensor". The rotation of two adjacent tensors occurs with small angles and therefore smoothly. The only exception to this can be seen at the upper right edge: The interpolated tensor $\boldsymbol{T}_{10,13}$ in the middle of $\boldsymbol{UM}$ and

  doi:10.5075/epfl-298799_978-2-9701614-0-0 published under CC BY-NC 4.0 license

$\boldsymbol{UR}$ behaves somewhat strangely as far as the behavior of the row is concerned. Instead of closing the estimated angle of 20° between the measured tensors to its left and right by a 10° change, this one rotates around the larger 170°. However, the tensor $\boldsymbol{MM}$ is also taken into account for the calculation of this tensor, even if weighted less strongly than $\boldsymbol{UM}$ and $\boldsymbol{UR}$. Furthermore, the behavior in this column looks much better than could be expected if the tensor had rotated in the other direction. In order to be able to approach quantitative error analyses and to better assess the interpolation behavior, one measured tensor of $\mathcal{T}_m$ was omitted in each case and also determined with the interpolation method. The visualization results are shown in the nine lower pictures in Figure 1. There are definite changes in the orientation course. For example, the behavior of $\boldsymbol{T}_{10,13}$ changes significantly when $\boldsymbol{UM}$ or $\boldsymbol{UR}$ are omitted.

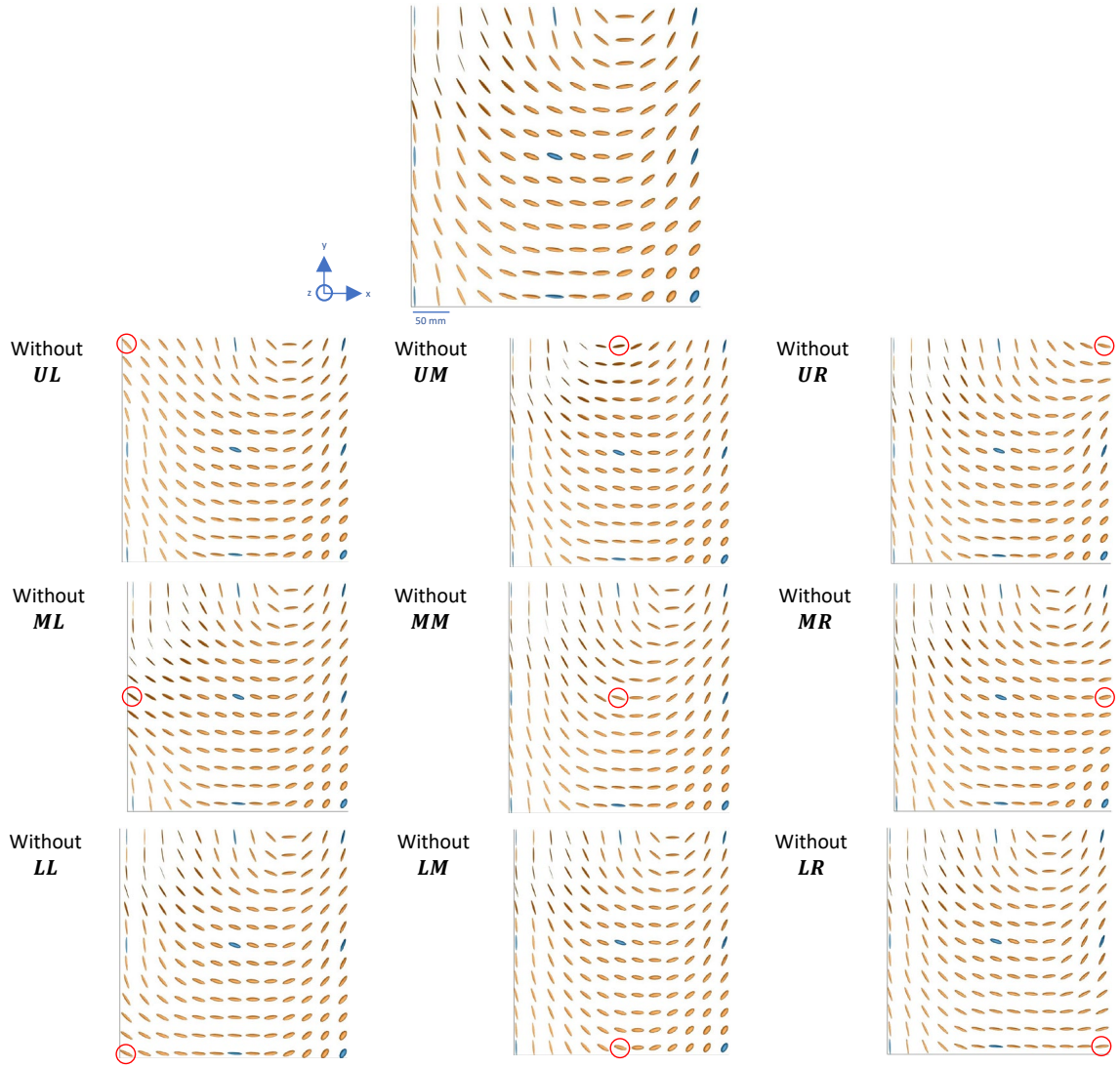

Figure 1. Picture at the top: Visualization of interpolated (orange) and measured (blue) tensors when using the decomposition-based interpolation method described in this paper. Lower nine pictures: Result when leaving one measured tensor out of the calculation and interpolating it instead respectively.

To obtain a quantitative error value, the Frobenius norm of the measured tensors and their respective interpolated substitutes was formed. The result can be seen in Figure 2. The rather

  doi:10.5075/epfl-298799_978-2-9701614-0-0 published under CC BY-NC 4.0 license

poorer interpolation at the left and upper edges and the relatively good performance in the middle of the plate (and lower right) are noticeable.

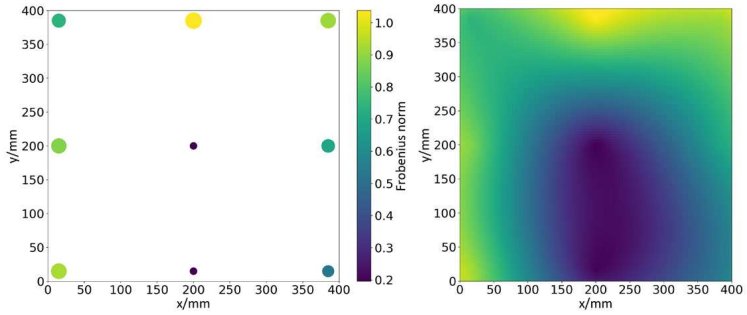

Figure 2. Visualization of the discontinuous (left image) and continuous (right image) error across the plate of the interpolated tensor in comparison to the measured one when leaving this specific tensor out of the computation. Value determined via Frobenius norm.

5. Discussion

Uneven height or dimensions of the plastificate and uneven temperatures in the tool could explain the curve in the orientation tensor field. The authors distinctively measured variations in both temperature and geometry, presumably causing the flow front to start prematurely in one edge. Furthermore, the plastificate is inserted in the mold manually, resulting in skewed/angular position of the plastificate when the press closes.

The interpolation behavior at the top right could be artificially prevented by restricting the possible angle. This could be implemented via comparing the results of the scalar products of the specific quaternions involved and taking the one providing the maximum scalar product. However, the authors tried to implement as little artificial restrictions as possible. Furthermore, as described before, the visual smoothness of rotation highly depends on whether one considers the row or the column course of rotation. In addition, the use of projectors instead of invariants might simplify the shape interpolation due to its uniqueness for a given tensor.

6. Conclusion

The implemented method provides for good macroscopic interpolation results for fiber orientation tensor fields interpolating measured FOT determined from microscopic X-ray computed tomography scans. Especially the observed isotropy behavior is satisfying. The quantitative error is higher towards the edges of the plate. Further research approaches should consist of testing this method with more sampling points (or with less of them being at the borders of the plate) and with plates that show different orientation behavior, as well as implementing a sensible angle restriction or using projectors. The use of a convolutional neural network instead of an algebraic solution could prevent the necessity of incorporating physical phenomena.

  doi:10.5075/epfl-298799_978-2-9701614-0-0

Acknowledgements

The research documented in this manuscript has been funded by the German Research Foundation (DFG) within the International Research Training Group “Integrated engineering of continuous-discontinuous long fiber reinforced polymer structures” (IRTG 2078). The support by the German Research Foundation (DFG) is gratefully acknowledged. Furthermore, the authors would also like to thank the Fraunhofer ICT for their support by providing the LFT plates, which were manufactured under the project leadership of Christoph Schelleis.

7. References

1. Advani SG, Tucker CL. The Use of Tensors to Describe and Predict Fiber Orientation in Short Fiber Composites. Journal of Rheology 1987; 31(8): 751–84.
2. Krause W, Henning F, Tröster S, Geiger O, Eyerer P. LFT-D — A Process Technology for Large Scale Production of Fiber Reinforced Thermoplastic Components. Journal of Thermoplastic Composite Materials 2003; 16(4): 289–302.
3. Terada M, Yamanaka A, Shimamoto D, Hotta Y, Shiraki K, Kimoto Y et al. Carbon fiber sampling method for determining the fiber length distribution. Advanced Composite Materials 2021; 30(sup1): 59–76.
4. Arsigny V, Fillard P, Pennec X, Ayache N. Log-Euclidean metrics for fast and simple calculus on diffusion tensors. Magn Reson Med 2006; 56(2): 411–21.
5. Gahm JK, Wisniewski N, Kindlmann G, Kung GL, Klug WS, Garfinkel A et al. Linear invariant tensor interpolation applied to cardiac diffusion tensor MRI. Medical image computing and computer-assisted intervention: MICCAI (International Conference on Medical Image Computing and Computer-Assisted Intervention) 2012; 15(Pt 2): 494–501.
6. Ennis DB, Kindlmann G. Orthogonal tensor invariants and the analysis of diffusion tensor magnetic resonance images. Magn Reson Med 2006; 55(1): 136–46.
7. Hiai F, Petz D. Riemannian metrics on positive definite matrices related to means. Linear Algebra and its Applications 2009; 430(11-12): 3105–30.
8. Sabiston T, Inal K, Lee-Sullivan P. Application of Artificial Neural Networks to predict fibre orientation in long fibre compression moulded composite materials. Composites Science and Technology 2020; 190: 108034.
9. Schultz T, Kindlmann GL. Superquadric glyphs for symmetric second-order tensors. IEEE Trans Vis Comput Graph 2010; 16(6): 1595–604.
10. Barmpoutis A, Vemuri BC, Shepherd TM, Forder JR. Tensor splines for interpolation and approximation of DT-MRI with applications to segmentation of isolated rat hippocampi. IEEE Trans Med Imaging 2007; 26(11): 1537–46.
11. Feldkamp LA, Davis LC, Kress JW. Practical cone-beam algorithm. Journal of the Optical Society of America A 1984; 1(6): 612–9.
12. Krause W, Henning F, Tröster S, Geiger O, Eyerer P. LFT-D — A Process Technology for Large Scale Production of Fiber Reinforced Thermoplastic Components. Journal of Thermoplastic Composite Materials 2003; 16(4): 289–302.
13. Pinter P, Dietrich S, Bertram B, Kehrer L, Elsner P, Weidenmann KA. Comparison and error estimation of 3D fibre orientation analysis of computed tomography image data for fibre reinforced composites. NDT & E International 2018; 95: 26–35.

  doi:10.5075/epfl-298799_978-2-9701614-0-0